JOURNAL OF VIROLOGY, Nov. 2011, p. 11242–11254 Vol. 85, No. 21
0022-538X/11/$12.00 doi:10.1128/JVI.05340-11

Canine Distemper Virus Infects Canine Keratinocytes and Immune Cells by Using Overlapping and Distinct Regions Located on One Side of the Attachment Protein▽

Johannes P. M. Langedijk,[2] Jozef Janda,[1] Francesco C. Origgi,[3] Claes Örvell,[4] Marc Vandevelde,[5] Andreas Zurbriggen,[1] and Philippe Plattet[1]*

Department of Clinical Research and Veterinary Public Health,[1] Division of Neurology,[5] and Centre for Fish and Wildlife Health (FIWI)-ITPA,[3] Vetsuisse Faculty, University of Bern, Bern, Switzerland; Innovation and Discovery Laboratory, Crucell Holland B.V., Archimedesweg 4-6, P.O. Box 2048 2301 CA, Leiden, The Netherlands[2]; and Laboratory of Clinical Virology, Karolinska University Hospital Huddinge, Stockholm, Sweden[4]

Received 8 June 2011/Accepted 8 August 2011

The morbilliviruses measles virus (MeV) and canine distemper virus (CDV) both rely on two surface glycoproteins, the attachment (H) and fusion proteins, to promote fusion activity for viral cell entry. Growing evidence suggests that morbilliviruses infect multiple cell types by binding to distinct host cell surface receptors. Currently, the only known *in vivo* receptor used by morbilliviruses is CD150/SLAM, a molecule expressed in certain immune cells. Here we investigated the usage of multiple receptors by the highly virulent and demyelinating CDV strain A75/17. We based our study on the assumption that CDV-H may interact with receptors similar to those for MeV, and we conducted systematic alanine-scanning mutagenesis on CDV-H throughout one side of the β-propeller documented in MeV-H to contain multiple receptor-binding sites. Functional and biochemical assays performed with SLAM-expressing cells and primary canine epithelial keratinocytes identified 11 residues mutation of which selectively abrogated fusion in keratinocytes. Among these, four were identical to amino acids identified in MeV-H as residues contacting a putative receptor expressed in polarized epithelial cells. Strikingly, when mapped on a CDV-H structural model, all residues clustered in or around a recessed groove located on one side of CDV-H. In contrast, reported CDV-H mutants with SLAM-dependent fusion deficiencies were characterized by additional impairments to the promotion of fusion in keratinocytes. Furthermore, upon transfer of residues that selectively impaired fusion induction in keratinocytes into the CDV-H of the vaccine strain, fusion remained largely unaltered. Taken together, our results suggest that a restricted region on one side of CDV-H contains distinct and overlapping sites that control functional interaction with multiple receptors.

Morbilliviruses belong to the subfamily *Paramyxovirinae* and include a number of highly virulent pathogens occurring worldwide, such as measles virus (MeV) in humans and the closely related canine distemper virus (CDV) in domestic and wild carnivores (13). The pathogenesis of MeV and CDV infections is remarkably similar. Notably, lymphoid tissue is the first site where viral replication occurs, correlating with severe immunosuppression. Subsequently, a variety of epithelial tissues, such as those present in the upper and lower respiratory tract, can be infected (16, 39). Finally, morbilliviruses may invade the central nervous system (CNS), potentially mediating severe neurological disorders. While the frequency of CNS complications in MeV infection remains marginal, they are very common in canine distemper, with the development of a demyelinating, multiple sclerosis-like disease (1, 2, 37).

In morbillivirus infection, the initial interaction with the host cell is governed by the envelope-anchored attachment protein (the H [hemagglutinin] protein), an essential viral component, which, assisted by the viral fusion protein, initiates cell entry and cell-to-cell spread by binding a host cell surface receptor (13, 41). The signaling lymphocyte activation molecule (CD150/SLAM) has been identified as a universal *in vivo* morbillivirus receptor (34, 36). SLAM expression in certain immune cells clearly correlates with the severe immunosuppression associated with MeV- and CDV-mediated cytolytic infection of lymphoid tissue (19, 35, 45). While SLAM is the only receptor identified to date that is used by wild-type morbillivirus strains, both cellular and functional data strongly support the existence of additional host cell surface molecules that allow viral entry and subsequent spread in a variety of organs and systems, notably in polarized epithelial cells (the presumptive receptor for MeV in polarized epithelial cells is referred to as EpR) (16, 30, 32, 33). Importantly, Leonard and colleagues recently reported that wild-type MeV infection of the airway epithelium through EpR was strictly required for the occurrence of viral shedding (16). The MeV H protein (MeV-H) exhibits a six-bladed (β1 to β6) β-propeller fold; each blade has four β-strands (S1 to S4) (Fig. 1A and B). Residues in MeV-H that support EpR-dependent plasma membrane fusion activity were identified; they cluster close to a small socket at the tip of a recessed groove created by β4 and β5 on one side of the β-propeller (16, 32) (Fig. 1C). Importantly, the identified EpR-docking site is located nearby, but clearly separated from residues previously determined to reg-

* Corresponding author. Mailing address: Department of Clinical Resarch and Veterinary Public Health, University of Bern, Bremgartenstrasse 109a, 3001 Bern, Switzerland. Phone: 4131 631 26 48. Fax: 4131 631 25 38. E-mail: philippe.plattet@vetsuisse.unibe.ch.

▽ Published ahead of print on 17 August 2011.

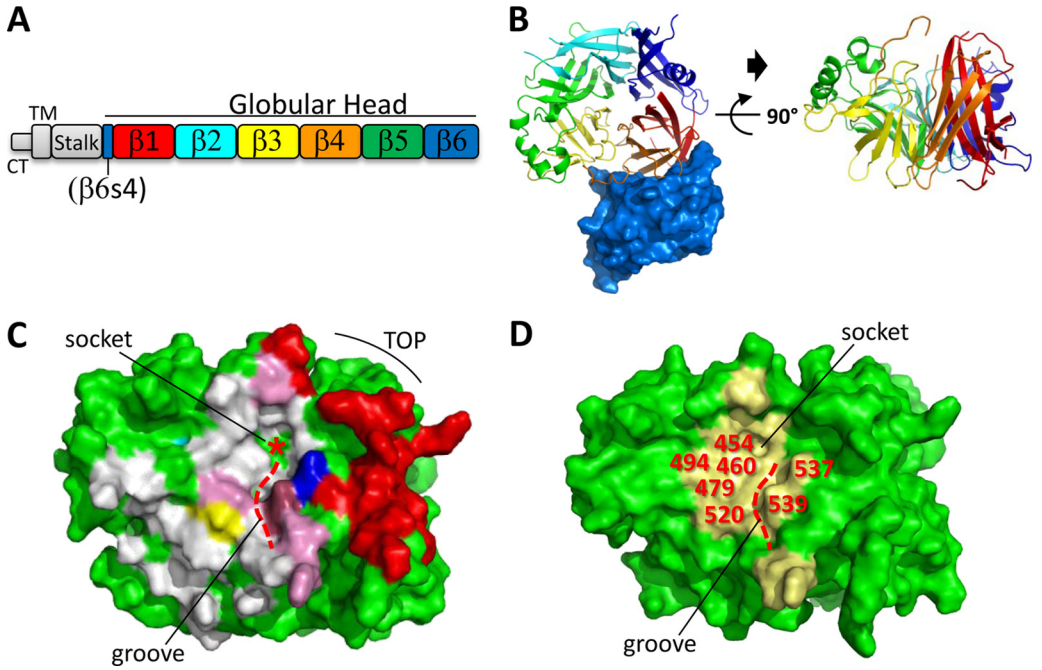

FIG. 1. CDV-H structural model and localization of residues selected for alanine-scanning mutagenesis. (A) Primary structure of the H protein. CT, cytoplasmic tail; TM, transmembrane region; β1 to β6, color-coded β-propeller blades 1 to 6. (B) (Left) Top view of MeV-H (cartoon) in complex with CD46 (surface representation; dark blue) (PDB code 3INB) (28). (Right) Side view of MeV-H/CD46 (with CD46 removed). The color coding of β-strands corresponds to that in panel A. (C) Surface representation of MeV-H, shown in the same orientation as that on the right side of panel B. The curved black line indicates the top of the MeV-H β-propeller structure. The small socket (red asterisk) that locates the tip of the recessed groove (dashed red line) is indicated. Red, residues recently documented to contact SLAM (11); white, residues reported in MeV-H to contact CD46 (28); pink, residues shown to contact both CD46 and SLAM. Residues that support EpR-dependent fusion activity (16, 32) are shown in different colors: residue 482 in yellow, residue 497 in cyan, residue 541 in dark blue, and residue 543 in raspberry. Residues 482, 541, and 543 are also part of the SLAM and CD46 binding site. (D) Surface representation of the CDV-H structural model (based on MeV-H/CD46 [PDB code 3INB]), shown in the same orientation as that of MeV-H in panel C. Yellow, residues selected for alanine-scanning mutagenesis (20 amino acids) that potentially interact with multiple receptors used by CDV. Positions of selected residues are labeled in red. The small socket and the recessed groove (dashed red line) are also indicated.

ulate SLAM-dependent fusion activity (Fig. 1C) (16, 32). Recent structural insights have confirmed that SLAM contacts MeV-H through multiple contacting sites. In addition, the cocrystal structure revealed that the socket and the recessed groove are also part of the H/SLAM interface (11). Thus, both structural and functional evidence supports the concept that a common face of the hemagglutinin acts as a multiple-receptor-binding domain (11, 16, 28, 32). On the other hand, there is no doubt that morbilliviruses can interact with cell receptors in a highly selective way (15–17, 30, 40). This implies that structurally subtle but functionally significant differences at the H/receptor interface, most likely crucial in controlling tissue-specific cell entry, do exist.

As in MeV infection, virulent CDV also invades epithelial and CNS tissues, which do not express SLAM (7, 8, 27, 44), suggesting the usage of other receptors. To gain further insight into CDV-mediated multiple-receptor usage, we used the virulent CDV strain A75/17, which was isolated directly from lymphoid tissues of a naturally CDV infected dog and, importantly, was never adapted to grow in any cell lines. This virus, for which efficient reverse genetics is available (26, 27), grows well in several primary canine cell cultures, where it closely reproduces the selective noncytolytic cell-to-cell spread seen *in vivo*. In this study, we propose that CDV-H may interact with receptors similar to those for MeV. To verify this notion, we conducted comprehensive structure-guided alanine-scanning mutagenesis on CDV-H throughout one side of the β-propeller that has been documented in MeV-H to bind multiple receptors (11, 28). The ability of mutants to cause cell-cell fusion in primary canine keratinocytes and canine SLAM-expressing cells was used as a measure of the efficiency of the H-receptor interaction.

Our biochemical and functional data identified 11 residues in CDV-H, clustering either at the center or along the rim of a recessed groove located on one side of the β-propeller structure, that selectively regulate fusion activity in keratinocytes without influencing SLAM-dependent fusion. Conversely, several CDV-H mutations that have been reported to abolish fusion and interaction with canine SLAM (46) also modulated fusion induction in keratinocytes. Intriguingly, when mutated residues shown to ablate fusion in keratinocytes were transferred to the CDV-H of the vaccine strain, fusion remained largely unaltered. Together, these results provide new insights concerning how CDV-H may interact with various receptors to regulate cell entry specificity, tropism, and pathogenesis.

MATERIALS AND METHODS

Cell cultures and viruses. 293T cells, Vero cells, Vero cells expressing the SLAM receptor (Vero-SLAM cells), and Vero-SLAM cells additionally engineered to express wild-type H (H^{wt}) (Vero-SLAM-H wt cells) were grown in

Dulbecco's modified Eagle's medium (Gibco, Invitrogen) with 10% fetal calf serum (FCS) at 37°C in the presence of 5% CO_2. Bsr-T7/5 cells were grown like Vero cells, except that the medium was supplemented with 2% FCS and 0.5 mg/ml of G418. Primary canine keratinocyte cultures were prepared as described previously (7, 27, 47). The recombinant vaccinia virus MVA-T7 was used for a quantitative cell-cell fusion assay and was obtained from B. Moss, NIH, Bethesda, MD. The recombinant A75/17-CDV strain and derivative mutants, containing an additional red fluorescent protein (RFP) gene, were amplified in Vero-SLAM cells.

Rescue of recombinant viruses. Recombinant viruses were generated as described previously (26, 43). Briefly, BsrT7 cells in 6-well plates were cotransfected with 2.5 μg of full-length cDNA of the relevant clones together with the expression vectors encoding the N, P, and L proteins (0.2, 0.2, and 0.05 μg, respectively). Two days posttransfection, the cells were transferred to petri dishes containing Vero-SLAM cells at 90% confluence. When cytopathic effect was obvious, cells were subjected to two cycles of freeze-thawing, and the supernatant was then cleared by centrifugation. The recombinant viruses were further amplified by two additional passages in Vero-SLAM cells. Stocks of viruses were titrated by a limiting dilution assay. To efficiently rescue SLAM-blind mutants, we used a previously described modified reverse-genetics system (44). Briefly, Vero cells constitutively expressing both the SLAM and H molecules were used for viral amplification (Vero-SLAM-Hwt).

Construction of expression plasmids. All single (and multiple) substitutions performed in pCI-Hwt^{eF} (derived from CDV strain A75/17 hemagglutinin [46]) and in pCI-HOP^{eF} (derived from CDV strain Onderstepoort hemagglutinin [46]) were carried out using the QuikChange Lightning site-directed mutagenesis kit (Stratagene). The pCI-H-SLAM-blind vectors have been described previously (46).

The plasmid containing the full-length cDNA copy of the A75/17-CDV genome (pA75/17^{red}) was first digested with MluI and BssHII. A small linker containing an additional transcription unit as well as two RsrII sites was generated by annealing two oligonucleotides and was subsequently cloned into the MluI/BssHII-cleaved pA75/17^{red} plasmid. Then the H Y539A gene was cleaved by digesting the pCI expression plasmid with RsrII and was subsequently cloned into the RsrII-cleaved full-length pA75/17^{red} plasmid. This procedure generated pA75/17^{red}/H-Y539A. Rescue of rA75/17^{red}/H-Y539A was performed as mentioned above. SLAM-blind H-bearing cDNA clones were generated in a similar way with the difference that the genes were first amplified by PCR from previously reported SLAM-blind expression vectors (46). These H genes additionally contain a FLAG tag sequence (DYKDDDDK) at their C-terminal regions. Rescue of SLAM-blind recombinant viruses was performed as mentioned above. All full-length genome sequences respect the rule of six and were confirmed by automated nucleotide sequence analysis.

Transfections and luciferase reporter gene content-mixing assay. Vero cells, in 6-well plates at 90% confluence, were cotransfected with 1.9 μg of the pCI-F^{wt} constructs (24), 1 μg of the various pCI-H plasmids, and 0.1 μg of pCI-RFP with 9 μl of Fugene HD (Roche) or with 1 μg of the various pCI-H plasmids in 24 wells with 3 μl of Fugene HD, according to the manufacturer's protocol. In some experiments, phase-contrast pictures were taken with a confocal microscope (FluoView FV1000; Olympus) 24 h posttransfection.

Primary canine epithelial keratinocytes, in 6-well plates at 70% confluence, were cotransfected with 1.9 μg of the pCI-F^{wt} constructs (24), 1 μg of the various pCI-H plasmids, and 0.1 μg of pCI-RFP (coding for red fluorescent protein) with 9 μl of Fugene HD (Roche). Although virulent CDV induces only rare syncytia in keratinocytes, we noticed that coexpression of both F^{wt} and H^{wt} glycoproteins in keratinocytes resulted in significant induction of cell-to-cell fusion activity. This could be explained by the fact that (i) in transient-transfection assays, fusion activity occurs in the absence of the matrix protein and/or that (ii) we used an engineered version of F that contains a heterotypic signal peptide; both characteristics have been reported to correlate with enhancement of fusion activity (23, 42).

The quantitative fusion assay was performed as described previously (18, 23). Briefly, Vero cells were cotransfected with the F and H expression plasmids and 0.1 μg of pTM-Luc (kindly provided by Laurent Roux, University of Geneva). In parallel, separate 6-well plates of Vero-SLAM cells or keratinocytes at 30% confluence were infected with MVA-T7 (31) at a multiplicity of infection (MOI) of 1. After overnight (O/N) incubation, the two cell populations were mixed. Two hours (Vero-SLAM cells) or 6 h (keratinocytes) later, the cells were lysed using Bright Glo lysis buffer (Promega), and the luciferase activity was determined using a luminescence counter (Perkin-Elmer Life Sciences) and the Britelite reporter gene assay system (Perkin-Elmer Life Sciences). In separate experiments, keratinocytes were infected with MVA-T7 at an MOI of 1. The protocol was the same as that employed when Vero-SLAM cells were used as target cells, except that both cell populations were cocultures 6 h prior to cell lysis.

We noticed high background values, ranging from 5 to 20%, when fusion was assessed quantitatively in epithelial keratinocytes (see Fig. 4A and B). This was presumably due to the relatively low efficiency of F/H-mediated syncytium formation in cells expressing KeR (the presumptive receptor used by CDV in canine keratinocytes), requiring a longer incubation of effector with target cells, as well as to the fact that small syncytia formed spontaneously in canine keratinocytes.

Western blotting. Western blotting was performed as described previously (23). Transfected cells were washed twice with cold phosphate-buffered saline (PBS) before the addition of 150 μl of lysis buffer (10 mM Tris [pH 7.4], 150 mM NaCl, 1% deoxycholate, 1% Triton X-100, 0.1% sodium dodecyl sulfate [SDS]) with Complete protease inhibitor (Roche Biochemicals). After incubation for 20 min at 4°C, the lysates were cleared by centrifugation at 5,000 × *g* for 15 min at 4°C, and the supernatant was first mixed with an equal amount of 2× Laemmli sample buffer (Bio-Rad) containing 100 mM dithiothreitol, then boiled at 95°C for 5 min, and finally fractionated on 8 or 10% SDS-polyacrylamide gels under denaturing conditions. The separated proteins were transferred to nitrocellulose membranes by electroblotting. The membranes were then incubated with the polyclonal rabbit anti-CDV F or H antisera (4) or a monoclonal antibody (MAb) against hemagglutinin (HA) (16B12; Covance). Following incubation with a peroxidase-conjugated secondary antibody, the membranes were subjected to enhanced chemiluminescence (ECL) by use of a kit (Amersham Pharmacia Biotech) according to the manufacturer's instructions.

F/H co-IP. At 24 h posttransfection, the cells were washed three times with cold PBS and were treated with DSP [dithiobis (succinimidylpropionate); final concentration, 1 mM in PBS; Sigma-Aldrich) for 30 min at room temperature (RT), followed by addition of Tris (pH 7.5)] to a final concentration of 20 mM for quenching (15 min at 4°C). Cells were subsequently lysed in radioimmunoprecipitation assay (RIPA) buffer (10 mM Tris [pH 7.4], 150 mM NaCl, 1% deoxycholate, 1% Triton X-100, 0.1% SDS) containing protease inhibitors (Complete mix; Roche) for 20 min on ice. Cleared lysates (20,000 × *g*; 20 min; 4°C) were incubated 3 h with the linear-epitope-recognizing anti-CDV-H MAb 1347 (20), followed by O/N incubation with immunoglobulin G-coupled Sepharose beads (GE Healthcare). The precipitates were washed three times each in coimmunoprecipitation (co-IP) buffer, followed by addition of 2× Laemmli sample buffer (Bio-Rad) containing 100 mM dithiothreitol. The samples were then subjected to Western blot analysis as described above using either the polyclonal anti-H or the anti-F antibody (4).

Flow cytometry. To determine the expression and conformations of the various H proteins specifically at the cell surface, Vero cells were first transfected with 1 μg of H expression plasmids. One day posttransfection, unfixed and unpermeabilized cells were washed twice with ice-cold PBS and were subsequently stained with one of the various MAbs (1:1,000) for 1 h at 4°C. Anti-CDV-H MAbs 1347, 3900, 2267, and PDVH11 have been described previously (20); anti-CDV-H MAb 1C42H11 was purchased from VMRD; and the anti-FLAG MAb (F3165) was purchased from Sigma-Aldrich. Staining with MAbs was followed by intensive washes with ice-cold PBS and incubation of the cells with an Alexa Fluor 488-conjugated secondary antibody (Invitrogen) (1:500) for 1 h at 4°C. Cells were washed 5 times with ice-cold PBS and were subsequently detached from the wells by the addition of PBS-EDTA (50 mM) for 30 min at 37°C. The mean fluorescence intensity of 10,000 cells was then measured by using a BD LSRII flow cytometer (Becton Dickinson).

Homology modeling. Homology modeling was performed using the sequence alignment of MeV-H and A75/17-CDV-H. Different models for CDV-H were generated based on the homologous template of the native H structure of MeV in complex with either CD46 (Protein Data Bank [PDB] code 3INB) or SLAM (PDB code 3ALZ) (11, 28). These cocrystal structures were chosen as templates because the interface of the receptors and hemagglutinin is slightly different from that for the uncomplexed crystal structures (5, 10). Models were built using the automated protein-modeling software provided by the SWISS-MODEL server (9, 22). According to the alignment, only a very few insertions and deletions were necessary to construct the model. The model was verified using WhatCheck and QMEAN4 (3, 12). The accuracy of the model was reasonable because of the high sequence similarity of CDV-H with the template (51% similarity and 38% identity). QMEAN Z scores were −4.2 and −4.7 for the two different templates used. Modeling was performed twice using the two separate MeV-H monomers, with very similar results. The two resulting CDV-H monomers were merged into a dimer. The CDV-H structural model presented in this report is based on MeV-H in complex with CD46 (PDB code 3INB).

RESULTS

Structure-guided design of CDV-H mutants. While residues interacting with SLAM in the morbillivirus H protein have already been mapped (17, 38, 40, 46), two studies recently documented the identification of MeV-H residues responsible for promoting fusion activity in polarized epithelial cells (16, 32). These clustered either near or within a recessed groove created by β-propeller blades 4 and 5 on one side of H (Fig. 1C) (16, 32). However, neither accurate quantitative data for the effect of the identified amino acids in modulating EpR-dependent or SLAM-dependent fusion activities nor assessment of the putative functions of surrounding nonconserved residues was documented (16, 32).

To better understand CDV-mediated entry into the cells of multiple tissues, we hypothesized that CDV-H may interact with receptors similar to those for MeV. Thus, we conducted comprehensive alanine-scanning mutagenesis of conserved and nonconserved residues of the entire region of A75/17-CDV-H that had been shown in MeV-H to contain multiple receptor-binding sites. For this purpose, we first generated a CDV-H structural model, based on the recently determined crystal structure of MeV-H in complex with CD46 (28). We then highlighted on the cocrystal structure of MeV-H/CD46 the residues that contact CD46 and SLAM as well as the amino acids putatively binding to EpR (Fig. 1C) (16, 32). Based on the former indications, we then selected 20 residues in CDV-H predicted to be surface exposed and encompassed within the region documented in MeV-H to bind multiple receptors (Fig. 1D). The residues within this region of CDV-H from the virulent A75/17 strain were replaced with alanine. Detection by flow cytometry of the C-terminally FLAG tagged H proteins (46) confirmed that all mutants except CDV-H I463A were properly expressed at the cell surface (not shown).

Identification of KeR-blind CDV-H mutants. We previously proposed the presence of a new, unidentified receptor in canine keratinocytes, because they are susceptible to virulent CDV infection even though they do not express SLAM (27). Although the EpR described for MeV-H on human polarized epithelial cells and the unidentified receptor for CDV-H on canine epithelial keratinocytes may be a common morbillivirus receptor, in this study we refer to the presumptive receptor used by CDV in canine keratinocytes as KeR.

We next assessed the abilities of all CDV-H mutants to promote fusion activity in keratinocytes. For this purpose, keratinocytes were transfected with the panel of H mutant-expressing plasmids in combination with the vector encoding the fusion protein, as well as a red fluorescent protein (RFP)-expressing plasmid for accurate fusion detection. Compared to H^{wt}, the P454A, L460A, L479A, I494A, L510A, Y520A, Y537A, and Y539A H mutants exhibited a complete lack of fusion activity in primary canine epithelial keratinocytes 2 days posttransfection (and therefore are referred to as KeR-blind mutants) (Fig. 2A). Moreover, the V478A, T496A, and I522A H mutants were characterized by induction of intermediate KeR-dependent fusion support activities (Fig. 2A). Thus, no fewer than 11 of the 20 targeted mutants were found to reduce KeR-dependent fusion significantly.

While all H mutants but one were surface exposed (not shown), we investigated whether the lack of fusion support ability in certain mutants correlated with overall conformational misfolding. For this purpose, several MAbs that recognize epitopes on the β-propeller were used to probe the conformation of KeR-blind H mutants (anti-CDV-H MAbs 2267, 1C42H11, and 3900 and anti-PDV [phocine distemper virus]-H11, which cross-reacts with CDV-H [20]). To take into consideration the subtle differences recorded in the cell surface expression of all H mutants, mean fluorescence intensities (MFI) measured by flow cytometry analyses with the anti-H MAbs were normalized to the MFI of surface expression obtained with the anti-FLAG MAb. Finally, the MFI obtained with the Hwt^{eF} construct was arbitrarily set to 100%. Figure 2B shows that no KeR-blind H mutants exhibited any significant alteration in their overall conformation, although only four MAbs were available to probe the CDV-H conformation.

Next, the receptor specificity of each H mutant generated was explored. For this purpose, KeR-blind H mutants were assessed for their abilities to mediate syncytium formation through the SLAM molecule. All KeR-blind H proteins were thus expressed in Vero-SLAM cells together with the fusion protein, and the efficiency of syncytium formation was monitored 24 h posttransfection. Strikingly, all KeR-blind H mutants expressed in Vero-SLAM cells induced cell-cell fusion with wild-type-like efficiency, suggesting that KeR-dependent fusion-regulatory residues were not involved in modulating SLAM-mediated fusion activity (Fig. 2C). These results also confirmed that the overall conformational state of KeR-blind H mutants remained functional in triggering the fusion protein.

Figure 3B demonstrates that all KeR-dependent fusion-modulating residues cluster within, or at the rim of, a recessed groove created by blades 4 and 5 on one side of the β-propeller, a domain also used by SLAM for interaction with H (Fig. 3A). This region corresponds to the location of the equivalent residues in MeV-H that are critical for binding to EpR (Fig. 1C). The center of the groove is composed almost exclusively of leucine, isoleucine, and tyrosine residues, suggesting that hydrophobic interactions might play a critical role in supporting an efficient KeR-H docking interaction.

Quantitative assessment of receptor usage by selected H mutants. To investigate the receptor usage of several KeR-blind H mutants in more detail, we accurately quantified their abilities to induce fusion in KeR^+ and $SLAM^+$ target cells in a well-established quantitative luciferase reporter gene content-mixing assay (18, 24, 25). Because Vero cells do not support fusion induction with A75/17-CDV F/H combinations, these cells were used as effector cells. Vero cells were thus transfected with CDV F/H mutants, and 1 day posttransfection, they were mixed with different target cells: either Vero-SLAM cells or KeR-expressing keratinocytes. In this series of experiments, we selected representative H mutants: three with recorded KeR-blind activity (the P454A, I494A, and Y539A mutants) and one that showed wild-type-like fusion support activity in KeR^+ cells (the Y543A mutant). Figure 4A validated the striking KeR-blind phenotype of the P454A, I494A, and Y539A H mutants, in contrast to the Hwt^{eF} construct or the Y543A H mutant. Also, a slight reduction in SLAM-dependent fusion promotion activity was recorded for the P454A and I494A H mutants. We noted, however, that both mutants also exhibited a slight decrease in surface expression (not

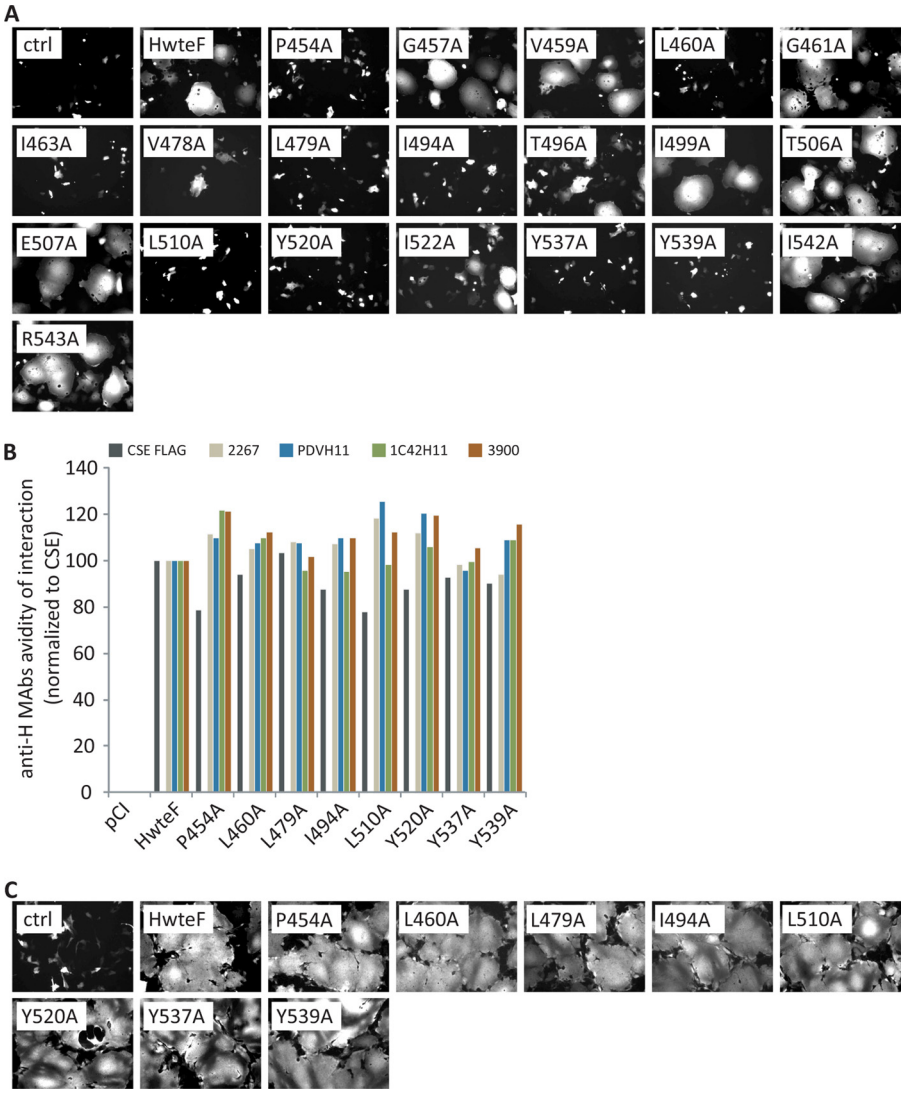

FIG. 2. Identification of KeR-regulating residues in CDV-H. (A) Syncytium formation after cotransfection of primary canine epithelial keratinocytes with plasmid DNA encoding various CDV-H proteins and F^{wt}. Mock-transfected cells received a plasmid encoding CDV-F^{wt} and an empty vector (pCI). In every experiment, the expression plasmid encoding RFP was cotransfected. Representative fields of view of fluorescence emission captured with a confocal microscope 24 h posttransfection are shown. (B) Probing of the potential conformational change in the various H mutants. The binding efficiencies of four conformational anti-H MAbs (2267, 1C42H11, 3900, and PDVH11) to the different H proteins expressed in Vero cells were assessed by flow cytometry. The binding avidity for each MAb was next calculated as follows: mean fluorescence intensities recorded with the anti-H MAbs were normalized to the levels obtained with the anti-FLAG MAb (to control for any surface expression differences between the various H mutants). Values were finally set to 100% for H^{wt}. Means from three independent experiments carried out in duplicate are shown. CSE, cell surface expression. (C) Syncytium formation after cotransfection of Vero-SLAM cells with plasmid DNA encoding various CDV-H proteins and F^{wt}. Mock-transfected cells received a plasmid encoding CDV-F^{wt} and an empty vector (pCI). In every experiment, the expression plasmid encoding RFP was cotransfected. Representative fields of view of fluorescence emission captured with a confocal microscope 24 h posttransfection are shown.

shown), which very likely contributed to the slight fusion promotion defect in $SLAM^+$ cells. In contrast, the Y539A H mutant, which completely lacked fusion promotion activity in KeR-expressing cells, retained a wild-type-like fusion support function in cells expressing SLAM (Fig. 4A).

Previously reported SLAM-blind H mutants were next assessed for their abilities to trigger fusion in KeR-expressing cells (we selected two single H mutants, the Y525A and R529A mutants; one triple mutant, the Y525A D526A R529A mutant; and one mutant, HSB, containing six mutated residues: D526A, I527A, S528A, R529A, Y547A, and T548A [46]). Consistent with previous results (46), all mutants were strongly defective in supporting fusion activity through the SLAM molecule, although single mutated proteins (especially the Y525A H mutant) retained minimal fusion activity (Fig. 4B). However, all SLAM-blind H proteins also exhibited a marked defect in promoting fusion in KeR-expressing cells (Fig. 4B). Only the Y525A H mutant exhibited less than a 50% deficiency in fusion promotion activity compared to that of the Hwt^{eF} construct in KeR^+ cells. We noted that HSB totally lost its

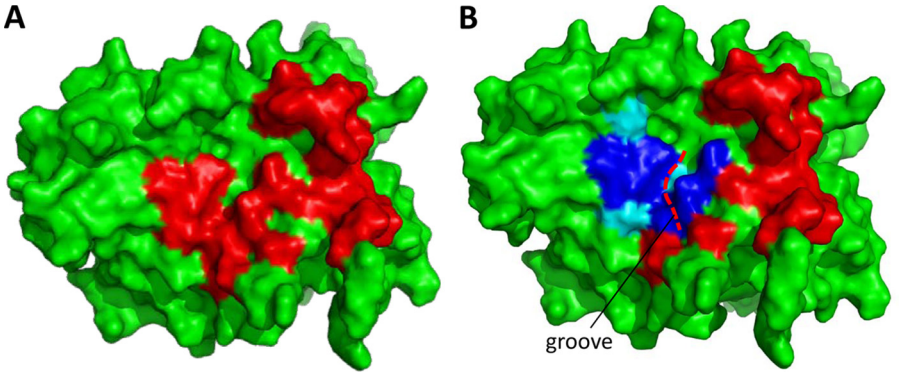

FIG. 3. Localization of residues identified in CDV-H that control functional interaction with KeR. Shown are surface representations of the CDV-H structural model in the same orientation as in Fig. 1D. (A) Red, residues in CDV-H that contact canine SLAM based on homology modeling with MeV-H and human SLAM (11). (B) Blue, residues in CDV-H mutation of which completely inhibits KeR-dependent fusion activity; cyan, residues in CDV-H mutation of which partially inhibits KeR-dependent fusion activity; red, residues in CDV-H that contact canine SLAM based on homology modeling with MeV-H and human SLAM (11). The recessed groove is also indicated (dashed red line).

fusion promotion activity in both KeR^+ and $SLAM^+$ target cells, suggesting that this mutant presumably is characterized by deficiencies in additional fusion support functions (i.e., F triggering and/or interaction with F) (Fig. 4B).

Taken together, our quantitative assessment of fusion activity revealed that truly selective KeR-blind H mutants could be generated. In contrast, SLAM-blind mutants were, to a certain extent, additionally interfering with fusion activity in KeR-expressing cells.

KeR-blind H mutants maintain a proper interaction with F. To investigate whether the KeR-dependent fusion-deficient phenotype of various H mutants was influenced by impaired functional interaction with F, we performed coimmunoprecipitation assays with total-cell lysates of F/H-transfected Vero cells. In this assay, cells were first treated 24 h posttransfection with the membrane-permeant cross-linker DSP and were subsequently lysed using the stringent RIPA buffer. F/H complexes were then immunoprecipitated (IP) using a linear-epitope-recognizing MAb (anti-H MAb 1347) so as to exclude any influence of slight H conformational modifications on IP efficiency. Lysates were finally subjected to Western blot analysis using a monoclonal anti-HA antibody (the F protein bears an HA tag fused C-terminally [4]).

Figure 4C demonstrates that omitting H from the transfection mixture resulted in the absence of F copurification. Strikingly, in the presence of DSP, functional F_1 subunits could readily be copurified with all mutated H proteins (Fig. 4C, coIP). To further confirm the specificity of the co-IP assay, we included as a control H 112 N-glyc, an H protein mutated at position 114 within the stalk domain so as to generate an additional *N*-glycan at position 112. This strategy was recently shown to prevent F-H interaction in MeV, presumably because this region in the stalk domain engages in a short-range interaction with F (6, 14, 21). While H 112 N-glyc retained normal cell surface expression and interaction with a soluble form of SLAM, it completely lost fusion promotion activity in Vero-SLAM cells (not shown), a phenotype that correlated with the absence of functional F_1 interaction (Fig. 4C, coIP). We noticed the presence of an unspecific band recognized by the anti-HA antibody in the control experiment, which comigrated with putative F_0 precursors (Fig. 4C, coIP), thereby precluding accurate identification of the latter antigenic material. We therefore focused our analysis on the cleaved F_1 subunit, which obviously represents the interaction of functional F proteins with H. Furthermore, total expression of the various H proteins was assessed in a direct IP assay, which revealed proper expression of the I494A and Y539A H mutants (Fig. 4C, IP). In contrast, the P454A substitution caused a slight decrease in overall H protein synthesis (Fig. 4C, IP). Finally, to investigate whether F was properly expressed in every combination, we performed immunoblotting from cell lysates taken prior to IP. The results indicated proper F expression in all transfected F/H combinations (Fig. 4C, TL) and thus validated our co-IP assay.

Importantly, while the I494A and Y539A H mutants exhibited wild-type-like interactions with F, F_1 was slightly less copurified when combined with the P454A H mutant (Fig. 4C, coIP). We noticed, however, that this mutant additionally exhibited a slight decrease in protein synthesis (Fig. 4C, TL). In summary, we concluded from these experiments that since the KeR-blind I494A and Y539A H mutants (i) interacted properly with functional F proteins, (ii) were efficiently transported to the cell surface (not shown), and (iii) were intrinsically functional for F triggering (Fig. 2C), the lack of fusion promotion observed in epithelial keratinocytes most likely correlates with a blockade of KeR-H interactions. In the case of the specific P454A H mutant, we cannot exclude the possibility that impairment of F-H functional interactions, in addition to reduced expression and subsequent limited surface targeting, may additionally contribute to the overall lack of fusion support ability.

Investigation of selective receptor usage by recombinant viruses. To confirm that KeR-blind hemagglutinins identified in the transient cell-cell fusion assay were also relevant in the context of a viral infection, we selected the H Y539A substitution and transferred it into the cDNA backbone of the virulent A75/17-CDV strain. The latter infectious clone additionally contains a supplementary transcription cassette coding for red fluorescent protein (27, 43, 44). The corresponding recombinant virus (recA75/17^{red}-H-Y539A) was successfully recov-

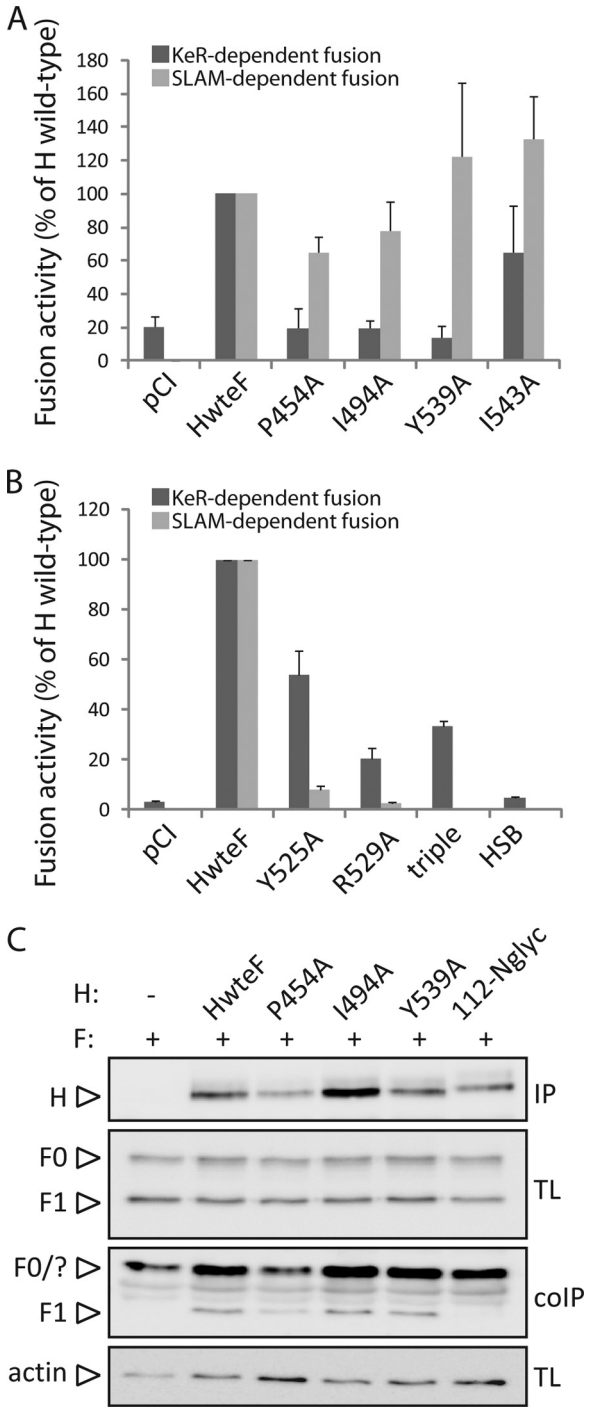

FIG. 4. Quantitative investigation of the selectivity of receptor-dependent fusion support deficiency for selected H mutants. (A) Assessment of KeR-dependent fusion-defective H mutants in a luciferase reporter gene content-mixing assay. Vero-SLAM cells or keratinocytes (target cells) were infected with MVA-T7 (MOI, 1). In parallel, a second population (Vero cells, used as effector cells) was transfected with the different H proteins, a plasmid encoding F^{wt}, and a plasmid containing the luciferase reporter gene under the control of the T7 promoter. Twelve hours after transfection, effector cells were mixed with target cells (either with Vero-SLAM cells or with keratinocytes) and were seeded into fresh plates. After 2.5 h (Vero-SLAM cells) or 6 h (keratinocytes) at 37°C, fusion was quantified by using a commercial luciferase-measuring kit. For each experiment, the value for the F^{wt}/H^{wt} combination was set to 100%. Means and standard deviations for three independent experiments carried out in duplicate are shown. (B) The experiment described for panel A was carried out with previously identified SLAM-dependent fusion-defective H mutants. (C) Assessment of interaction of H with functional F proteins. To stabilize the F-H interactions, transfected Vero cells were treated, or not, with the membrane-permeant cross-linker DSP. Then Vero cells cotransfected with the various H-expressing plasmids or an empty plasmid (pCI) together with F^{wt}-expressing plasmids or pCI were lysed with the stringent RIPA buffer, followed by immunoprecipitation (IP) of H with a linear-epitope-recognizing anti-H MAb (1347) and treatment with protein G-Sepharose beads. Proteins were then boiled and subjected to immunoblotting using a polyclonal anti-HA antibody to detect the F antigenic materials (F contains an HA tag fused at its C-terminal region [24]). Co-IP F proteins were detected by comparison with F present in the lysates prior to IP by immunoblotting using a polyclonal anti-F antibody (TL). As a control, total H proteins, obtained by direct immunoprecipitation with the MAb mentioned above, were revealed by immunoblotting using a polyclonal anti-H antibody (IP). Finally, as a loading control, total expression of the actin protein in each sample is shown (actin).

ered and was subsequently inoculated into $SLAM^+$ and KeR^+ target cells. Consistent with results obtained in the transient cell-cell fusion assay, recA75/17^{red}-H-Y539A was characterized by a complete inability to infect KeR-expressing cells, as demonstrated by the absence of red fluorescence emission monitored by fluorescence microscopy for 6 days after the initial infection (Fig. 5A, top center). In contrast, the wild-type virus (recA75/17^{red}) elicited efficient cell-to-cell transmission in the absence of obvious syncytium formation (Fig. 5A, top left). Importantly, both viruses induced massive syncytium formation in Vero-SLAM cells, thereby confirming the generation of an efficient selective KeR-blind recombinant canine distemper virus (Fig. 5A, bottom left and center).

Since the wild-type virus mediated a noncytolytic cell-to-cell type of infection in canine epithelial keratinocytes, and thus was potentially regulated by very specific mechanisms, we sought to investigate whether both viral cell entry and lateral cell-to-cell spread were defective in cells infected with the KeR-blind recombinant virus. With this aim, we passaged the virus in Vero-SLAM-Hwt cells, a derivative Vero cell clone engineered to constitutively express both the SLAM and H^{wt} molecules (44). This strategy allowed *trans*-complementation of viral particles by wild-type H proteins and, thus, discrimination between cell entry efficiency (virus-cell fusion) and lateral cell-to-cell spread (cell-cell fusion). After 6 days of incubation, epithelial keratinocytes inoculated with the H^{wt}-complemented KeR-blind virus (recA75/17^{red}-H-Y539A/Hcomp) exhibited only a single or very few compact clusters of infected cells (Fig. 5A, top right). This contrasted with wild-type CDV-infected cells, where foci with more than 100 infected cells were always captured (Fig. 5A, top left). Furthermore, as anticipated, recA75/17^{red}-H-Y539A/Hcomp induced massive cell-cell fusion in Vero-SLAM cells (Fig. 5A, bottom right). Combined, these results indicated that residue Y539, located within the recessed groove of CDV hemagglutinin, controls both KeR-dependent virus-cell fusion and lateral cell-cell fusion activity.

SLAM-blind recombinant viruses were next generated to investigate whether the partial defect recorded in the transient fusion assay in KeR-expressing cells would also be observed in

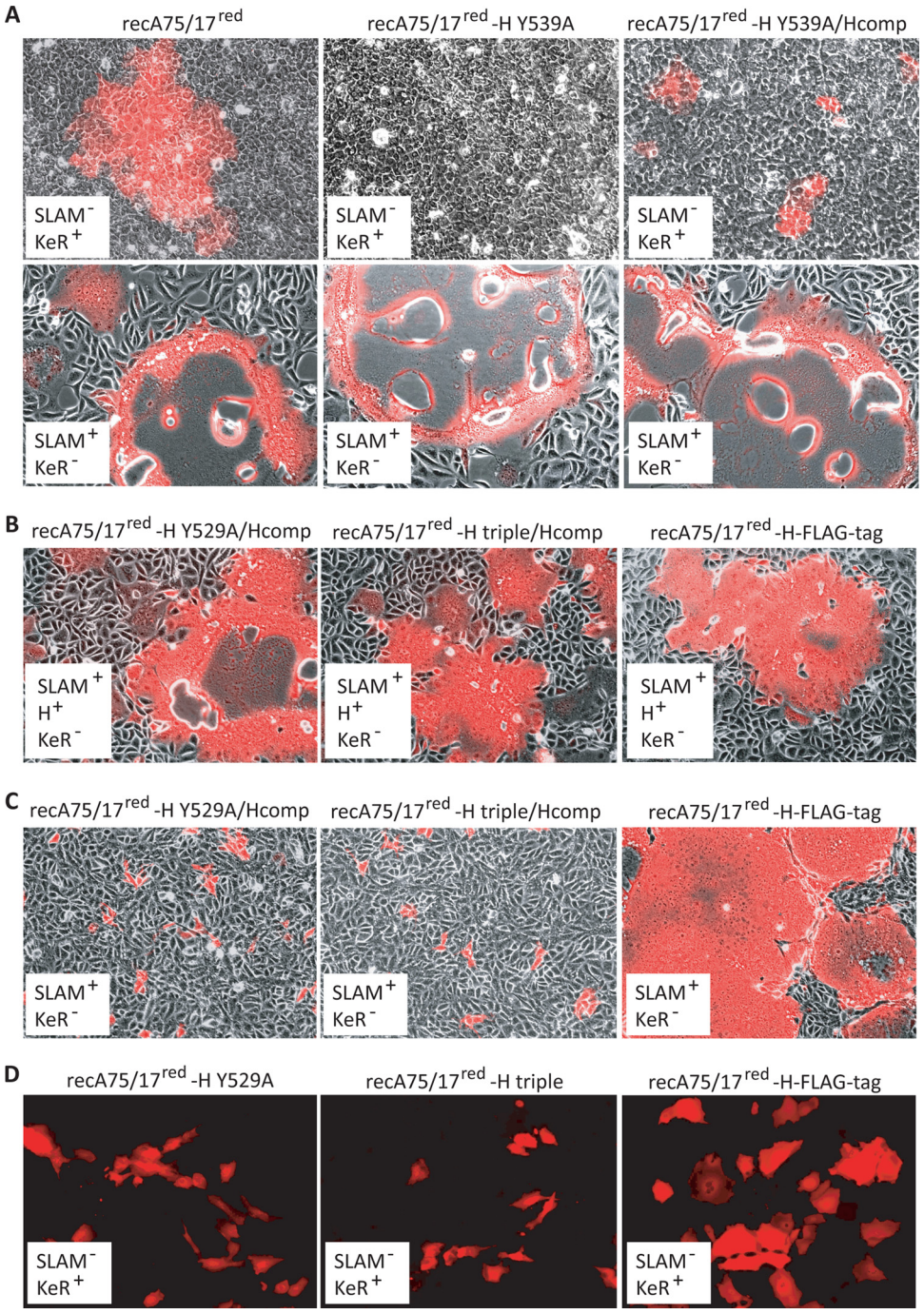

FIG. 5. Assessment of the selective receptor usage of several recombinant CDVs. (A) Keratinocytes or Vero-SLAM cells were infected with recA75/17^{red}, recA75/17^{red}-H Y539A, or recA75/17^{red}-H Y539A/Hcomp at an MOI of 0.01. Seven days (keratinocytes) or 1 day (Vero-SLAM cells) postinfection, infected cells were screened for red fluorescence emission by confocal laser fluorescence microscopy. Phase-contrast images merged with fluorescence emission images of representative fields of view are shown. (B) Vero-SLAM-Hwt cells were infected with recA75/17^{red}-H-FLAG-tag, recA75/17^{red}-H Y529A/Hcomp, or recA75/17^{red}-H triple/Hcomp at an MOI of 0.01. One day postinfection, infected cells were screened for red fluorescence emission by confocal laser fluorescence microscopy. Phase-contrast images merged with fluorescence emission images of representative fields of view are shown. (C) The experiment described for panel B was carried out in Vero-SLAM cells. (D) The experiment described for panel B was carried out in keratinocytes. Fluorescence emission images of representative fields of view are shown.

the context of a complete viral infection. We selected the single R529A substitution (H 529A) as well as the triple H mutation (Y525A, D526A, and R529A [H triple]), which we transferred separately into the A75/17-CDV molecular clone. To amplify the rescued viruses, we used the Vero-SLAM-Hwt cell line to complement the defect of the mutated H proteins in *trans*. Using this approach, H-SLAM-blind recombinant viruses that additionally contained the H^{wt} protein in their envelopes were

successfully recovered. Furthermore, the H proteins were engineered to contain a FLAG tag fused to the C-terminal region. As a control of viral replication, all three viruses were then inoculated into Vero-SLAM-Hwt cells. All three recombinant viruses (recA75/17^{red}-H-529A/Hcomp, recA75/17^{red} H-triple/Hcomp, and recA75/17^{red}-H-FLAG-tag) exhibited strong cytopathic effect in these cells by inducing the formation of large syncytia (Fig. 5B). In Vero-SLAM cells, however, only recA75/17^{red} H-FLAG-tag mediated significant cell-cell fusion (Fig. 5C, right), whereas both SLAM-blind mutants (recA75/17^{red} H-529A/Hcomp and recA75/17^{red} H-triple/Hcomp), though clearly entering into the cells, exhibited strong impairment in subsequent lateral spread (Fig. 5C, left and center). This phenotype of infection validated the defect of both specific recombinant viruses in promoting fusion activity through the SLAM molecule. Finally, the recombinant viruses were inoculated into primary canine epithelial keratinocytes in order to investigate receptor usage selectivity. Strikingly, all three recA75/17-CDV strains could spread in KeR-expressing cells, though to different extents. Indeed, both SLAM-blind viruses were characterized by a slight defect in infecting keratinocytes compared to recA75/17^{red}-H-FLAG-tag (Fig. 5D).

Taken together, these results confirmed the data obtained in the transient cell-cell fusion assay, which documented partial inhibition of the promotion of fusion activity through the presumptive KeR by SLAM-blind H protein mutants.

Transfer of KeR-blind mutations into the vaccine strain hemagglutinin protein did not alter the fusion support function in Vero cells. Vero cells are of epithelial origin and were employed, at least in part, to generate the CDV vaccine strain Onderstepoort (OP-CDV). We reasoned that the hemagglutinin of CDV Onderstepoort (HOP) may promote efficient binding to Vero cells and canine keratinocytes by using the newly identified KeR-binding site. However, the fact that the wild-type A75/17 virus, which efficiently infects KeR-expressing keratinocytes, does not replicate efficiently in Vero cells argues for the existence of an additional mode(s) of interaction between HOP and an unidentified receptor. To distinguish between these possibilities, we transferred some of the KeR-blind mutations identified into HOP (Fig. 6A to E; see Fig. 1D for their localization) and tested the abilities of derivative mutants to trigger fusion in both cell types. Interestingly, all mutated proteins maintained fusion support ability both in keratinocytes and in Vero cells, though, for some mutants, to a lesser extent than did the nonmutated HOP protein (Fig. 6B). This indicated either that the KeR-binding site in HOP is partially different from that in H^{wt} or that HOP binds an undetermined receptor expressed in Vero cells (of monkey origin), which is additionally present in primary epithelial keratinocytes (of canine origin). In Vero cells, only two HOP mutants (the I494A and Y520A mutants) were characterized by an impaired fusion support function (Fig. 6C). However, assessment of cell surface expression revealed that both H mutants were defective in intracellular transport competence (Fig. 6A).

We next generated double, triple, and quadruple mutants bearing combinations of the single substitutions mentioned above. Strikingly, all mutated H proteins retained very efficient fusion support activity in both Vero cells and keratinocytes (Fig. 6D and E). We noticed that although the quadruple H mutant was characterized by strong impairment of intracellular transport competence (Fig. 6A), substantial cell-cell fusion was nevertheless reproducibly promoted in transfected cells.

Taken together, these data suggest that HOP binds KeR either in a different way, using different critical residues within or around the recessed groove, or through a distinct region(s). Alternatively, this uncharacterized receptor-binding site might have arisen through viral adaptation to cultured cells and might represent indirect evidence for the existence of an additional unidentified receptor that would be expressed both in Vero cells and in epithelial keratinocytes.

DISCUSSION

In the present study, we have explored the molecular basis of CDV-mediated multiple-receptor usage. The targeting of specific receptors and associated cellular changes ultimately determine the outcome of infection and the potential of inducing severe disease.

In a recently revised model of MeV-induced pathogenesis, it was postulated that infection of human polarized epithelial cells through an unidentified receptor (EpR) requires prior viral replication in immune cells expressing the universal morbillivirus receptor CD150/SLAM (16). This model illuminated the subtle regulation of multiple-receptor usage by morbilliviruses, not only determining which cell types are infected but also at what time point they are targeted during a course of infection. Past and recent reports provided evidence that one face on the side of the MeV-H globular head domain was involved in binding to multiple receptors (11, 28, 29, 38, 41). In order to shed light on CDV-mediated multiple-receptor usage, we inoculated the neurovirulent A75/17-CDV strain into different cell types that may potentially selectively express two different CDV receptors: SLAM and the putative KeR. This strategy was combined with a systematic, structure-guided, site-directed mutational analysis, which allowed us to identify 11 residues in CDV-H that regulated KeR-dependent fusion activity. Since the general strategy used in MeV-H to identify regulating amino acids was based on the selection of conserved residues within the *Morbillivirus* genus, it was not surprising that some of the residues identified in CDV-H were similar to those found in MeV-H (L482, F483, P497, Y541, and Y543 [MeV-H amino acid numbering]) (Fig. 7) (16, 32). Even though the conserved amino acid P497 was not mutated in our study, since the majority of the side chain is buried, its neighboring residue T498 (I494 in CDV-H) was demonstrated to contribute strongly to KeR-dependent fusion control. The other four residues (L482, F483, Y541, and Y543) were demonstrated in CDV-H to govern fusion activity through KeR. In addition to these five residues, we identified six well-conserved amino acids that controlled KeR-dependent fusion (P454, L460, T496, L510, Y520, and L522 [CDV-H amino acid numbering]) (Fig. 7). Remarkably, when mapped on the CDV-H structural model, these 11 residues cluster either within or along the rim of a recessed groove located on one side of the β-propeller (Fig. 3). The location of this cluster of residues in CDV-H is exactly equivalent to that of the region in MeV-H that is presumably involved in EpR binding (Fig. 1C). These data led us to speculate that the presumptive canine KeR and the human EpR (the pu-

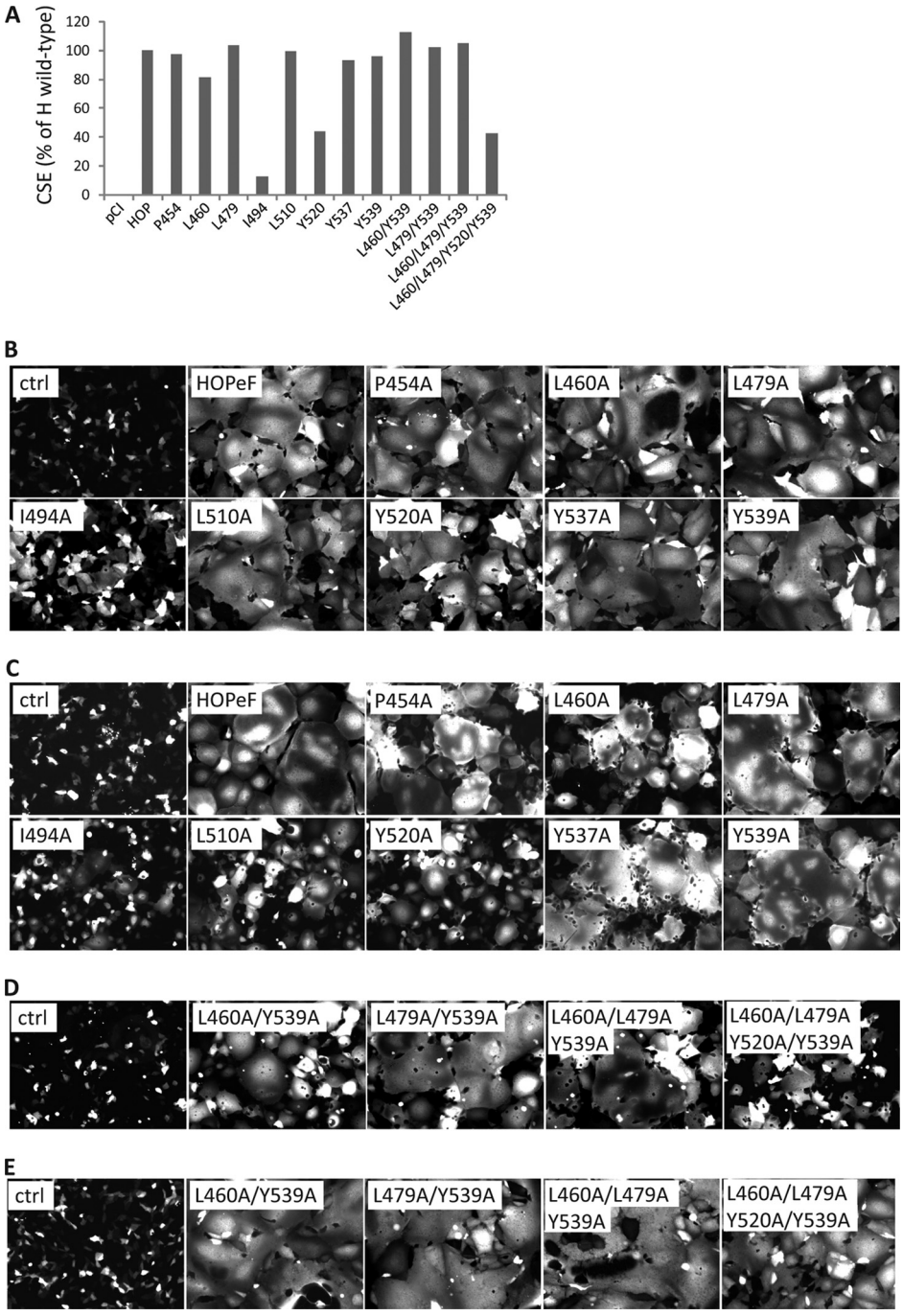

FIG. 6. Transfer of selected KeR-blind mutations into HOP does not alter fusion support activity. (A) Cell surface expression (CSE) of the various HOP^{cF} (HOP bearing a FLAG tag fused to the C-terminal region) mutants. The CSE of each H protein was determined by measuring the binding activity of each to the anti-FLAG MAb by flow cytometry. pCI, empty vector. Means from three experiments carried out in duplicate are shown. (B) Syncytium formation after cotransfection of keratinocytes with plasmid DNA encoding various CDV-HOP mutants and FOP. All CDV-HOP proteins additionally bear a C-terminal FLAG tag sequence (CDV-HOP^{cF}). Mock-transfected cells received a plasmid encoding CDV-FOP and an empty vector (pCI). In every experiment, the expression plasmid encoding RFP was cotransfected. Representative microscopic fields of view of fluorescence emission captured by confocal microscopy 24 h posttransfection are shown. (C) The experiment described for panel B was carried out in Vero cells. (D) The experiment described for panel B was carried out with HOP variants bearing multiple mutations. (E) The experiment for which results are shown in panel D was carried out in Vero cells.

tative receptor used by MeV in polarized airway epithelial cells) may be a common universal cell surface receptor targeted by morbilliviruses for entry into epithelial cells. However, it is possible that each morbillivirus efficiently uses only its own species-specific epithelial cell receptor, thereby limiting cross-species infection.

Residues in MeV-H previously shown to regulate SLAM-dependent fusion support activity (I194, Y529, D530, and

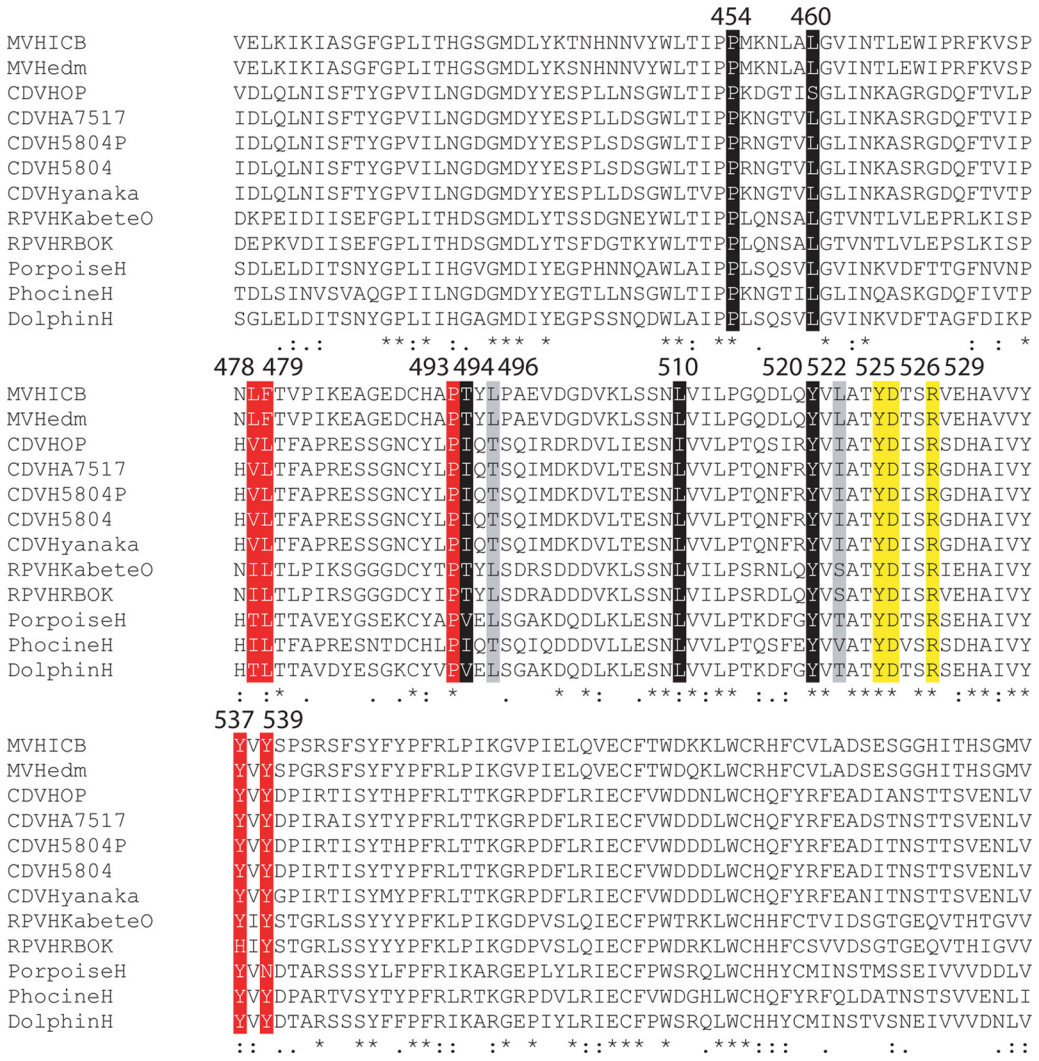

FIG. 7. Sequence alignment of the relevant region within the H proteins of various morbilliviruses. GenBank accession numbers for each virus sequence are as follows: AB016162.1 (measles virus strain ICB), AF266288.1 (measles virus strain Edmonston), AF305419.1 (canine distemper virus strain Onderstepoort), AY386316.1 (canine distemper virus strain A75/17), BAA01203.1 (canine distemper virus strain 5804P), AY386315.1 (canine distemper virus strain 5804), D85755.1 (canine distemper virus strain Yanaka), X98291.3 (rinderpest virus strain Kabete O), Y18816.1 (rinderpest virus strain K), FJ648457.1 (porpoise morbillivirus strain IRL88), FJ648456.1 (phocine distemper virus strain DK02), and NC_005283.1 (dolphin morbillivirus). Below the sequences, stars indicate identical residues, and colons indicate semiconserved residues. CDV-H residues regulating SLAM-dependent fusion (Y525, D526, and R529) are highlighted in yellow. CDV-H residues regulating KeR-dependent fusion are shown against a black (for residues shown in this study, if mutated, to fully ablate KeR-dependent fusion) or a gray (for residues shown, if mutated, to partially influence KeR-dependent fusion) background. Amino acid numbering corresponds to the CDV-H sequence. Residues shown in MeV-H to regulate EpR-dependent fusion are highlighted in red; among these five amino acids, residues 478, 479, 537, and 539 inhibit EpR/KeR-dependent fusion activity both in MeV-H and in CDV-H, whereas residue 493, if mutated, was reported to fully ablate EpR-dependent fusion only in MeV-H (this residue was not mutated in CDV-H in this study due to the low probability that it is surface exposed).

R533) were recently documented to influence EpR-dependent fusion as well (15). In the latter report, only a single SLAM-blind H mutant (the R533A mutant) was suggested to support wild-type-like EpR-dependent fusion promotion activity, although only qualitative data were presented (15). This notion prompted us to assess accurately, in a quantitative manner, the effect of SLAM-blind CDV H mutants in promoting fusion in KeR-expressing cells, as well as that of KeR-blind CDV H mutants in mediating fusion activity in SLAM-expressing cells. Strikingly, while KeR-blind H mutants retained their full ability to fuse SLAM-expressing cells and therefore seemed truly selective, all our tested SLAM-blind H mutants also partially interfered with fusion activity induced through KeR. This was not only observed in a transient cell-cell fusion assay but also confirmed in the context of a complete viral infection. These findings support the concept of a common region in one face of the morbillivirus H protein containing multiple overlapping receptor-binding sites. Remarkably, according to the recently determined crystal structures of the MeV-H/CD46 and MeV-H/SLAM complexes (11, 28), the critical residues for EpR binding overlap with the footprints of both CD46 and SLAM, although in the case of SLAM, the residues that do not overlap

and are located closer to the top of the side of the β-propeller are more important for binding (11). The impact of some mutations on both SLAM and KeR fusion promotion suggest that in CDV-H also, the receptor binding sites may overlap at (or close to) the recessed groove. Thus, based on the very close proximity of amino acids in H, mutation of which abrogates KeR/EpR-dependent fusion, and residues influencing CD46-dependent fusion in MeV-H, we hypothesize that, as with the D′D loop of CD46 (the docking domain of CD46 within the recessed groove [11]), a protruding domain of KeR (and of EpR) may be required in order to dock deeply into the recessed groove of the morbillivirus H protein to control functional interactions. Moreover, based on the results illustrating our inability to generate fully selective SLAM-blind CDV-H mutants, we suggest that an additional domain(s) within H must be essential to allow proper interaction with KeR. Pending identification of the receptor expressed in keratinocytes, followed by cocrystallization of this receptor bound to CDV-H, it is tempting at this stage to speculate that KeR (and presumably EpR with MeV-H) may share common docking interactive domains identified for both CD46 and SLAM. Indeed, in addition to the plug structure protruding from KeR docking in the recessed groove, KeR may extend its binding interface toward the top of the H head domain, where crucial residues controlling SLAM interaction reside (Fig. 1C) (11).

Direct comparison between the MeV-H/CD46 and MeV-H/SLAM modes of interaction indicates that in SLAM, residues are not forming a plug that penetrates deeply into the groove akin to the D′D loop of CD46 (11, 28). Intriguingly, while mutation of SLAM residues 72 to 76, which cover the recessed groove on the side of the MeV-H β-propeller, was recently shown to inhibit interaction with MeV-H (11), mutation of the corresponding contacting residues in MeV-H does not (16, 32). Thus, in contrast to the H-EpR and H-CD46 (for MeV) functional interactions, we hypothesize that no essential docking interaction occurs between SLAM and the center of the groove in MeV-H. In contrast, mutating residues 72 to 76 in SLAM may trigger long-range effects that may cause misfolding of one (or any) of the nearby binding sites, resulting in deficient MeV-H–SLAM association. This would rationally explain why mutation of residues at the center of the groove selectively abolishes EpR-dependent fusion, though these residues are involved in the SLAM-binding interface. This hypothesis may also be true for the selective KeR-blind CDV-H mutants with regard to the canine SLAM molecule. However, further investigations are required to verify this notion.

Interestingly, while both structural and functional data reported for MeV or CDV consistently illuminated an overlapping region on one of the faces of H as a multiple-receptor-binding domain, our results concerning receptor usage of the H protein derived from the tissue culture-attenuated CDV strain (HOP) suggest an additional mode of binding. When mutations in residues that had been shown to be critical for KeR-dependent fusion activity in the context of the wild-type H protein were transferred to HOP, fusion activities were not substantially altered either in KeR-expressing cells or in Vero cells. This finding suggests that HOP either binds to KeR in a different mode or via a different binding site or binds to an additional unidentified receptor. It is tempting to speculate that KeR binding was indeed abolished and that fusion activity was promoted through interaction with the unidentified receptor, which may be expressed in multiple cell types. Binding to this still uncharacterized receptor might well be a consequence of viral adaptation to cell cultures, as observed for MeV-H and CD46. While more studies are needed to clarify this notion, this observation suggests that confounding factors may be introduced into receptor interaction studies when CDV strains that have been passaged in cell cultures are used.

In summary, the results presented in this study provide further evidence that a common region located on one face of CDV-H is involved in KeR- and SLAM-binding activity. Our data suggest that KeR binds at the center of a recessed groove created by blades 4 and 5 on one side of the β-propeller and extends its interaction toward the top of the propeller, close to residues reported to contact SLAM (11). Furthermore, the similarity of our findings to those reported for MeV supports the view that the interaction of morbilliviruses with different cellular receptors is likely controlled by a tightly regulated usage of overlapping and unique stabilizing receptor-docking sites that reside in close proximity within the same face of the attachment protein.

ACKNOWLEDGMENTS

We are grateful to Patrick Salmon, Laurent Roux, Dominique Garcin, and Veronika von Messling for having provided the pRRL lentivirus plasmid system, the pTM-Luc plasmid, the RFP gene, and the Vero-SLAM cells, respectively. We also thank Jürgen Schneider-Schaulies for helpful comments on the manuscript.

This work was supported by the Swiss National Science Foundation (reference no. 310030_132887; to P.P.).

REFERENCES

1. **Appel, M. J.** 1969. Pathogenesis of canine distemper. Am. J. Vet. Res. **30:**1167–1182.
2. **Beineke, A., C. Puff, F. Seehusen, and W. Baumgartner.** 2009. Pathogenesis and immunopathology of systemic and nervous canine distemper. Vet. Immunol. Immunopathol. **127:**1–18.
3. **Benkert, P., M. Biasini, and T. Schwede.** 2011. Toward the estimation of the absolute quality of individual protein structure models. Bioinformatics **27:** 343–350.
4. **Cherpillod, P., K. Beck, A. Zurbriggen, and R. Wittek.** 1999. Sequence analysis and expression of the attachment and fusion proteins of canine distemper virus wild-type strain A75/17. J. Virol. **73:**2263–2269.
5. **Colf, L. A., Z. S. Juo, and K. C. Garcia.** 2007. Structure of the measles virus hemagglutinin. Nat. Struct. Mol. Biol. **14:**1227–1228.
6. **Corey, E. A., and R. M. Iorio.** 2007. Mutations in the stalk of the measles virus hemagglutinin protein decrease fusion but do not interfere with virus-specific interaction with the homologous fusion protein. J. Virol. **81:**9900–9910.
7. **Engelhardt, P., M. Wyder, A. Zurbriggen, and A. Grone.** 2005. Canine distemper virus associated proliferation of canine footpad keratinocytes in vitro. Vet. Microbiol. **107:**1–12.
8. **Grone, A., M. G. Doherr, and A. Zurbriggen.** 2004. Canine distemper virus infection of canine footpad epidermis. Vet. Dermatol. **15:**159–167.
9. **Guex, N., and M. C. Peitsch.** 1997. SWISS-MODEL and the Swiss-PdbViewer: an environment for comparative protein modeling. Electrophoresis **18:**2714–2723.
10. **Hashiguchi, T., et al.** 2007. Crystal structure of measles virus hemagglutinin provides insight into effective vaccines. Proc. Natl. Acad. Sci. U. S. A. **104:**19535–19540.
11. **Hashiguchi, T., et al.** 2011. Structure of the measles virus hemagglutinin bound to its cellular receptor SLAM. Nat. Struct. Mol. Biol. **18:**135–141.
12. **Hooft, R. W., G. Vriend, C. Sander, and E. E. Abola.** 1996. Errors in protein structures. Nature **381:**272.
13. **Lamb, R. A., and G. D. Parks.** 2007. *Paramyxoviridae*: the viruses and their replication, p. 1449–1496. *In* D. M. Knipe et al. (ed.), Fields virology, 5th ed. Lippincott Williams & Wilkins, Philadelphia, PA.
14. **Lee, J. K., et al.** 2008. Functional interaction between paramyxovirus fusion and attachment proteins. J. Biol. Chem. **283:**16561–16572.
15. **Leonard, V. H., G. Hodge, V. J. Reyes-Del, M. B. McChesney, and R. Cattaneo.** 2010. Measles virus selectively blind to signaling lymphocytic ac-

tivation molecule (SLAM; CD150) is attenuated and induces strong adaptive immune responses in rhesus monkeys. J. Virol. **84:**3413–3420.
16. **Leonard, V. H., et al.** 2008. Measles virus blind to its epithelial cell receptor remains virulent in rhesus monkeys but cannot cross the airway epithelium and is not shed. J. Clin. Invest. **118:**2448–2458.
17. **Navaratnarajah, C. K., et al.** 2008. Dynamic interaction of the measles virus hemagglutinin with its receptor signaling lymphocytic activation molecule (SLAM, CD150). J. Biol. Chem. **283:**11763–11771.
18. **Nussbaum, O., C. C. Broder, and E. A. Berger.** 1994. Fusogenic mechanisms of enveloped-virus glycoproteins analyzed by a novel recombinant vaccinia virus-based assay quantitating cell fusion-dependent reporter gene activation. J. Virol. **68:**5411–5422.
19. **Ono, N., H. Tatsuo, K. Tanaka, H. Minagawa, and Y. Yanagi.** 2001. V domain of human SLAM (CDw150) is essential for its function as a measles virus receptor. J. Virol. **75:**1594–1600.
20. **Orvell, C., H. Sheshberadaran, and E. Norrby.** 1985. Preparation and characterization of monoclonal antibodies directed against four structural components of canine distemper virus. J. Gen. Virol. **66**(Pt 3):443–456.
21. **Paal, T., et al.** 2009. Probing the spatial organization of measles virus fusion complexes. J. Virol. **83:**10480–10493.
22. **Peitsch, M. C.** 1996. ProMod and Swiss-Model: Internet-based tools for automated comparative protein modelling. Biochem. Soc. Trans. **24:**274–279.
23. **Plattet, P., et al.** 2007. Signal peptide and helical bundle domains of virulent canine distemper virus fusion protein restrict fusogenicity. J. Virol. **81:**11413–11425.
24. **Plattet, P., et al.** 2009. Conserved leucine residue in the head region of morbillivirus fusion protein regulates the large conformational change during fusion activity. Biochemistry **48:**9112–9121.
25. **Plattet, P., et al.** 2005. The fusion protein of wild-type canine distemper virus is a major determinant of persistent infection. Virology **337:**312–326.
26. **Plattet, P., et al.** 2004. Recovery of a persistent canine distemper virus expressing the enhanced green fluorescent protein from cloned cDNA. Virus Res. **101:**147–153.
27. **Rivals, J. P., P. Plattet, C. Currat-Zweifel, A. Zurbriggen, and R. Wittek.** 2007. Adaptation of canine distemper virus to canine footpad keratinocytes modifies polymerase activity and fusogenicity through amino acid substitutions in the P/V/C and H proteins. Virology **359:**6–18.
28. **Santiago, C., M. L. Celma, T. Stehle, and J. M. Casasnovas.** 2010. Structure of the measles virus hemagglutinin bound to the CD46 receptor. Nat. Struct. Mol. Biol. **17:**124–129.
29. **Schneider, U., F. Bullough, S. Vongpunsawad, S. J. Russell, and R. Cattaneo.** 2000. Recombinant measles viruses efficiently entering cells through targeted receptors. J. Virol. **74:**9928–9936.
30. **Shirogane, Y., et al.** 2010. Epithelial-mesenchymal transition abolishes the susceptibility of polarized epithelial cell lines to measles virus. J. Biol. Chem. **285:**20882–20890.
31. **Sutter, G., M. Ohlmann, and V. Erfle.** 1995. Non-replicating vaccinia vector efficiently expresses bacteriophage T7 RNA polymerase. FEBS Lett. **371:**9–12.
32. **Tahara, M., et al.** 2008. Measles virus infects both polarized epithelial and immune cells by using distinctive receptor-binding sites on its hemagglutinin. J. Virol. **82:**4630–4637.
33. **Takeda, M., et al.** 2007. A human lung carcinoma cell line supports efficient measles virus growth and syncytium formation via a SLAM- and CD46-independent mechanism. J. Virol. **81:**12091–12096.
34. **Tatsuo, H., N. Ono, K. Tanaka, and Y. Yanagi.** 2000. SLAM (CDw150) is a cellular receptor for measles virus. Nature **406:**893–897.
35. **Tatsuo, H., N. Ono, K. Tanaka, and Y. Yanagi.** 2000. The cellular receptor for measles virus: SLAM (CDw 150). Uirusu **50:**289–296. (In Japanese.)
36. **Tatsuo, H., N. Ono, and Y. Yanagi.** 2001. Morbilliviruses use signaling lymphocyte activation molecules (CD150) as cellular receptors. J. Virol. **75:**5842–5850.
37. **Vandevelde, M., and A. Zurbriggen.** 2005. Demyelination in canine distemper virus infection: a review. Acta Neuropathol. **109:**56–68.
38. **Vongpunsawad, S., N. Oezgun, W. Braun, and R. Cattaneo.** 2004. Selectively receptor-blind measles viruses: identification of residues necessary for SLAM- or CD46-induced fusion and their localization on a new hemagglutinin structural model. J. Virol. **78:**302–313.
39. **von Messling, V., D. Milosevic, and R. Cattaneo.** 2004. Tropism illuminated: lymphocyte-based pathways blazed by lethal morbillivirus through the host immune system. Proc. Natl. Acad. Sci. U. S. A. **101:**14216–14221.
40. **von Messling, V., et al.** 2005. Nearby clusters of hemagglutinin residues sustain SLAM-dependent canine distemper virus entry in peripheral blood mononuclear cells. J. Virol. **79:**5857–5862.
41. **von Messling, V., G. Zimmer, G. Herrler, L. Haas, and R. Cattaneo.** 2001. The hemagglutinin of canine distemper virus determines tropism and cytopathogenicity. J. Virol. **75:**6418–6427.
42. **Wiener, D., et al.** 2007. Synergistic inhibition in cell-cell fusion mediated by the matrix and nucleocapsid protein of canine distemper virus. Virus Res. **129:**145–154.
43. **Wiener, D., M. Vandevelde, A. Zurbriggen, and P. Plattet.** 2010. Investigation of a unique short open reading frame within the 3′ untranslated region of the canine distemper virus matrix messenger RNA. Virus Res. **153:**234–243.
44. **Wyss-Fluehmann, G., A. Zurbriggen, M. Vandevelde, and P. Plattet.** 2010. Canine distemper virus persistence in demyelinating encephalitis by swift intracellular cell-to-cell spread in astrocytes is controlled by the viral attachment protein. Acta Neuropathol. **119:**617–630.
45. **Yanagi, Y.** 2001. The cellular receptor for measles virus—elusive no more. Rev. Med. Virol. **11:**149–156.
46. **Zipperle, L., et al.** 2010. Identification of key residues in virulent canine distemper virus hemagglutinin that control CD150/SLAM-binding activity. J. Virol. **84:**9618–9624.
47. **Zurbriggen, A., and M. Vandevelde.** 1983. Canine distemper virus-induced glial cell changes in vitro. Acta Neuropathol. **62:**51–58.